AIMS Materials Science, 8(3): 416–433.
DOI: 10.3934/matersci.2021026
Received: 09 March 2021
Accepted: 23 May 2021
Published: 31 May 2021

http://www.aimspress.com/journal/Materials

Research article

DOE-based experimental investigation and optimization of hardness and corrosion rate for Cu–x%Al_2O_3 as processed by powder metallurgy

Omar Bataineh*, Abdullah F. Al-Dwairi, Zaid Ayoub, and Mohammad Al-Omosh

Department of Industrial Engineering, Jordan University of Science & Technology, P.O. Box 3030, Irbid 22110, Jordan

* **Correspondence:** Email: omarmdb@just.edu.jo.

Abstract: Copper alumina (Cu–x%Al_2O_3) was prepared from micro-sized powder particles through the powder metallurgy (PM) process. Experimental runs were designed according to the design of experiments (DOE) methodology to investigate the effect of alumina concentration and sintering time on the hardness and corrosion rate of the powdered composite. Four sintering times were tested (1, 2, 3, and 4 h) in combination with different levels of alumina concentration (1 wt%, 3 wt%, 6 wt%, and 10 wt%). Given the narrow range of the sintering temperature for copper alumina, this temperature was fixed at 900 °C, whereas the compaction pressure was set at 300 MPa. Collected data were analysed based on the analysis of variance (ANOVA) approach and complemented with microscopic analysis. Optimization techniques were used to identify the optimal settings of sintering time and alumina concentration for the PM composite.

Keywords: powder metallurgy; copper alumina; optimization; design of experiments; ANOVA

1. Introduction

Copper alumina is considered a successful example of metal matrix composites (MMC), where a ceramic addition improves strength and stiffness along with the high conductivity and toughness of the base metal [1–3]. While copper is an outstanding electrical and thermal conductor, alumina acts as a hard and thermally stable constituent that hinders dislocation movements within the lattice [4]. Given the relatively low cost of preparing and processing copper alumina, it has been used in

important applications such as disc brakes [5], electrical switches and connectors [6], high-power Light-Emitting Diode (LED) lamps [7], and high-field pulsed electromagnets [8].

The properties and characteristics of copper alumina composites largely depend on their preparation method, constituents' content, and setup of the relevant process variables. Various methods have been used to prepare copper alumina composites. Some of the methods depend on the principle of forming a porous medium of alumina that is infiltrated with copper. Tang et al. [7] fabricated copper alumina composite substrates used for high-power LED lamps through freeze-tape casting and infiltration. Their procedure included dipping a porous alumina substrate (1.5 mm thick) in a slurry of titanium, placing a copper sheet on top of the alumina substrate, which are then put together in an oven at 1100 °C for 1–5 h. Using scanning electronic microscopy (SEM), the rate of copper infiltration in the substrates was found to increase as sintering time, temperature, and Ti content were increased. Sang et al. [9] prepared copper alumina composites using alumina foam. Then they used the expendable casting process to infiltrate the foam with molten copper. Their work showed that the bending strength is proportional to the ceramic fraction, whereas the electrical conductivity and wear rate are inversely proportional. Winzer et al. [10] studied the wear behavior of copper alumina in terms of the ligament diameter and the copper content, which was controlled by using different alumina slurries. As the amount of copper increased, wear increased and hardness decreased, except where the cyclic tribo-layer behavior occurred. Hardness was highest when the copper ligament diameter was 30 μm.

Another method for preparing copper alumina composites is through the reduction of copper oxide (CuO) using aluminum in a ball mill [11]. Rajesh Kumar and Amirthagadeswaran [12] used high energy ball milling to synthesize nano-Al_2O_3 reinforced copper composite. Different weight percentages of alumina (5, 10, and 15 wt%) were examined. Corrosion tests using linear potentio-dynamic polarization tester and pin-on-disc wear tests were then used. Corrosion and wear values were best at 10 wt% and 15 wt% alumina, respectively. Eddine et al. [13] used the same method to produce nanostructured Cu–5 vol% Al_2O_3 composites, but the composites were sintered by pulsed electric current. The presence of nano-Al_2O_3 was found effective in the pinning of the grain boundaries, which limited grain growth and contributed to the bulk strength of the material.

In certain applications, copper alumina is used in the form of a coating, which requires different methods of synthesis. Mohammadi et al. [14] used solution combustion synthesis to produce nano Cu-Al_2O_3 composite coatings on copper substrates. The process used copper and aluminum nitrates as oxidizers, urea as source of fuel, and graphite as inhibitor. Their results revealed that the hardness and wear resistance were dependent on the ratio of urea-to-nitrates. Wang et al. [15] prepared copper alumina coatings by electrophoretic deposition and electroplating. Electrophoretic deposition was used to produce thin films of alumina, which are then plated and impregnated by copper through electroplating. Using SEM to examine the layered composite, alumina particles were found embedded within the copper matrix. Lim et al. [16] investigated surface roughness and surface pre-conditioning effects on the adhesion strength between copper and alumina layers in integrated circuits (IC) and multi-chip modules (MCM). They determined that heat treating substrates of alumina at 500 °C for 1 h was needed to eliminate excess moisture trapped inside the porosities. Increasing surface roughness by an average value of 500 nm, the adhesive strength was found to increase by more than 50%. This was explained by the 10% increase that occurred in the actual surface area of contact between the copper and alumina substrates.

Despite of the different methods of synthesis used for copper alumina, powder blending followed by sintering remains the most widely used one as it is easier to use, lower cost, and give more control over concentration of composite's constituents compared to other methods [12]. Qiao et al. [17] used powder blending and sintering to prepare a composite powder of copper/alumina/carbon-nanotubes (CNTs). At 0.5 wt% additions of alumina and CNTs, the tensile strength of copper/alumina/CNTs composite was higher by 43% than that of copper/alumina. Sadoun et al. [18] studied the effect of silver coated alumina on the microhardness of Al_2O_3 reinforced copper alumina nanocomposites fabricated using powder blending and sintering. The hardness of samples was found to increase with increasing alumina content. Their results showed that microhardness was maximum at 10 wt% of Al_2O_3 content. Rajkovic et al. [19] studied pre-alloyed copper powder to which 0.5 wt% aluminum and 0.6 wt% alumina was added. The composite was prepared by mechanical alloying and oxidation. The alumina particles were found to increase the micro-hardness of the composite. The formation of aluminum oxide precipitates from the pre-alloyed copper was an additional factor contributing to the hardening effect of the composite. Yousif and Moustafa [20] fabricated Cu–20 wt% Al_2O_3 composites using either Cu-coated alumina powders or by powder blending. The Cu-coated alumina composite was lower in electrical resistivity and coefficient of thermal expansion, and 25% higher in Brinell hardness compared to those made from blended powders. Korać et al. [21] prepared copper alumina composites with 1, 1.5 and 2 wt% Al_2O_3 using thermochemical synthesis, followed by mechanical alloying and sintering. The results showed that hardness decreased overall with the increase in alumina concentration, except when alumina concentration was below 1 wt%. Zheng et al. [22] prepared copper alumina using three successive steps: mechanical alloying, hydrogen sintering and explosive compaction with three explosion-induced pressures (2, 4, and 6 GPa). Hardness was found to increase with the explosion-induced pressure.

The goal of this study is to identify the optimal settings of sintering time and alumina concentration in terms of their effect on hardness and corrosion rate of Cu–x%Al_2O_3 composite as synthesized by the very common powder blending and sintering method. This investigation is motivated by the wide range of alumina percentages that have been tried in the research field using this method, which may have variable effects on the composite properties. Sintering time is also another important factor that is associated with powder blending and sintering method, thus it will be included in this study. Statistical ANOVA will be applied to reach conclusions that are statistically significant. Besides, response optimization will be performed to determine the levels of alumina weight percentage and sintering time at which hardness and corrosion rate are optimal.

2. Materials and methods

Factorial experiments were designed in this work according to the design of experiments (DOE) methodology [23]. Given the factors under study are the alumina concentration and sintering time, a two-factor four-level full factorial design with three replicates ($4^2 \times 3$) was used. This requires a total of 48 experimental runs to be conducted. These runs were carried out in a completely randomized order to minimize the effect of other nuisance factors that may occur during the test runs [24]. Weight percentages of 1%, 3%, 6%, and 10% were considered for the alumina concentration in this study. Higher concentrations were not used because of the noticeable negative impact of very high alumina concentrations on thermal and electrical conductivities of the copper alumina composites [25].

Sintering time was varied at 1, 2 3, and 4 h at a constant temperature of 900 °C. Below are further details on the raw materials used, preparation procedure, and tests conducted.

2.1. Materials

An electrolytic copper powder that is supplied by CHEMLAB Co., England was used. The powder was 99.8% in purity, and its particles were three dimensional (3D) and irregular in shape. The alumina powder used was produced by Albemarle Corporation, USA. It was α-type, spherically shaped, and 99.8% in purity. Photos for two samples of the copper and alumina powders are shown in Figure 1. The alumina powder is much finer than the copper powder. The size distribution of the two powders is represented in Figure 2. It can be seen from Figure 2 that the D10, D50 and D90 for copper are 13 μm, 40 μm, and 65 μm, respectively; and for alumina are 2 μm, 5 μm, and 7 μm, respectively. This difference in size leads to a higher specific surface area for the alumina powder relative to the copper powder. More of the characteristics of the copper and alumina powders are listed in Table 1.

Figure 1. Photo images for two samples of: (a) copper powder, and (b) alumina powder (both at X5 optical magnification).

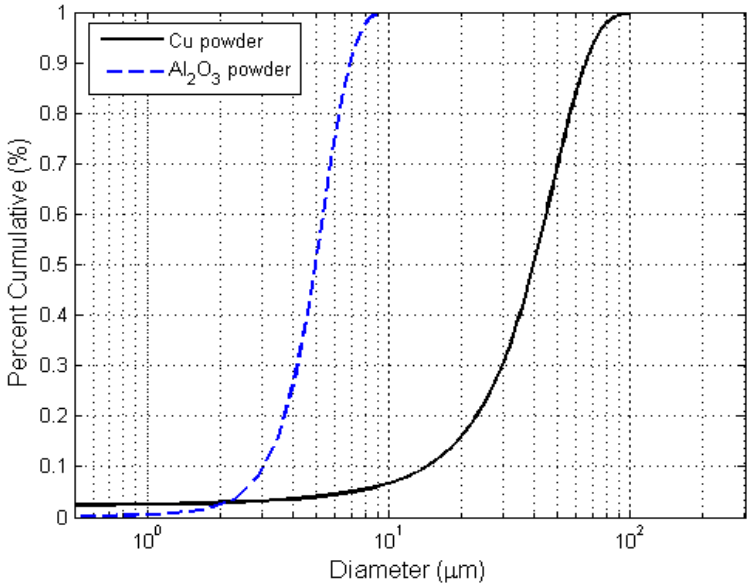

Figure 2. Size distribution of copper and alumina powders.

Table 1. Characteristics of copper and alumina powders.

Characteristic	Copper powder	Alumina powder
Powder type	electrolytic	A-type
Composition by weight	99.8% Cu	99.8% Al_2O_3
	<0.30% O_2	<0.10% Na_2O
	<0.02% Fe	<0.05% CaO
	<0.05% Pb	<0.04% Fe_2O_3
	<0.05% NHO_3	<0.08% SiO_2
Apparent density (g/cm^3)	2.35	0.7
Flow rate (s/50 g)	31	24
Melting temperature (°C)	1084	2054

2.2. Compaction and sintering

The powders of copper and alumina were mechanically stirred in cylindrical glass bottles for a period of 5 min to ensure the blend homogeneity. Then, a proper amount of the blend was used to fill a cylindrical die cavity of 17 mm in diameter. An upper punch was then used to compact the powder blend, which is supported from the lower side by the ejector pin, as shown in Figure 3. A compaction pressure of around 300 MPa was applied. After compaction, the now solid blend (called green compact) is ejected from the mold cavity using the ejector pin. All green compacts produced were approximately 25 mm long, which is controlled by providing the right amount of powder in the filling stage. Since the green compact is fragile and has a relatively low density (called green density), it was then sintered in an oven at a temperature of 900 °C for different time durations. No vacuum or inert gas was used in the sintering process, although this is preferable since it minimizes metal oxidation.

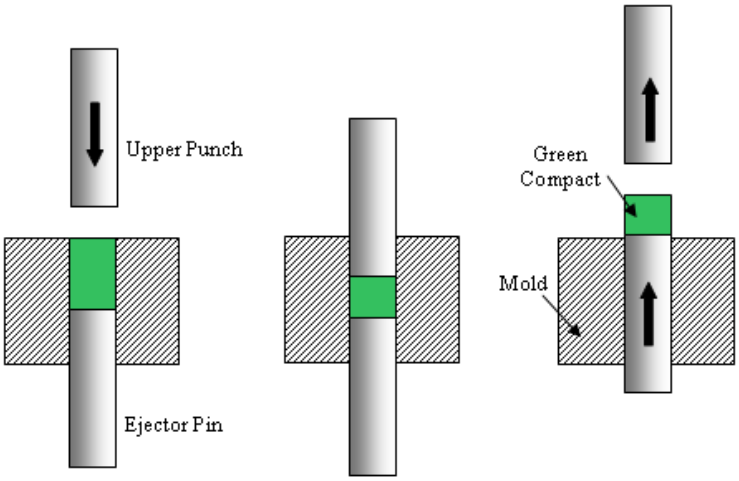

Figure 3. Powder compaction stages (from left to right): filling, compaction, and ejection.

2.3. Hardness and corrosion tests

Vickers hardness tests were applied according to ASTM E384 standard using a universal hardness testing machine manufactured by Indentec Litmited, an ISO 17025 UKAS accredited hardness calibration lab. Hardness readings were taken for the copper alumina specimens that have been compacted and sintered. Each hardness reading was based on the average of three measurements for a given specimen. After hardness readings were done, corrosion tests were carried out by immersing the specimens in a bath of hydrochloric acid (HCl) for four hours. Knowing the mass of a specimen before and after immersion, the weight loss (W) was then calculated. The average corrosion rate (CR) could then be calculated in units of mm/y from the weight loss according to Eq 1 as:

$$CR = \frac{8760W}{\rho AT} \tag{1}$$

where ρ is the sintered specimen density in g/mm^3, which is calculated from Eq 2 as the ratio of the specimen mass (M) to the volume of the cylindrical specimen of length (L) and diameter (D) according to:

$$\rho = \frac{4M}{\pi D^2 L} \tag{2}$$

T is the exposure time of the specimen in hours, and A is the initial apparent surface area of the specimen in mm^2, which is given by Eq 3 as:

$$A = \pi D\left(L + \frac{D}{2}\right) \tag{3}$$

Both L and D were measured twice at two orthogonal orientations for each specimen.

3. Results and discussion

The experimental results in terms of sintered density, Vickers hardness, weight loss, and corrosion rate are listed in Table 2. The sintered density is plotted against the sintering time, as shown in Figure 4. This figure shows that the sintered density increases with sintering time up to a peak point at approximately 3 h after which the density remains steady.

Vickers hardness is represented using a 3D surface plot, as shown in Figure 5. This plot is generated with MATLAB® using a spline interpolation fit of the data. Another way of representing the Vickers hardness data is by plotting the mean Vickers hardness against either alumina weight percentage or sintering time, as shown in Figure 6. Careful examination of Figures 5 and 6 reveal that the increase in alumina concentration overall increases hardness, although the change in hardness locally between the alumina concentrations of 3 wt% and 6 wt% is relatively small. The increase in sintering time has a tub-shape effect on hardness, as it decreases initially then it goes up. On average, the effect of sintering time on hardness is small when compared to that of the alumina concentration, as it lacks an increasing or decreasing trend. Similarly, corrosion rate data are represented using a 3D surface plot and means plot, respectively, as shown in Figures 7 and 8. It can be seen from these figures that the corrosion rate increases modestly initially then it begins to decrease as the alumina concentration increases. The increase in sintering time has a strong decreasing effect on corrosion rate, especially after 2 h of sintering.

Table 2. Experimental results at different alumina concentrations and sintering times.

Alumina content (wt%)	Sintering time (h)	Sintered density (g/cm^3)	Vickers hardness (MPa)	Weight loss (g)	Corrosion rate (mm/y)
1	1	6.684	605	2.636	0.00551
1	2	6.802	332	0.610	0.00125
1	3	6.850	582	0.805	0.00164
1	4	6.863	586	0.796	0.00162
3	1	6.593	685	2.976	0.00631
3	2	6.685	516	0.763	0.00159
3	3	6.744	676	0.984	0.00204
3	4	6.736	712	0.736	0.00153
6	1	6.362	616	1.616	0.00355
6	2	6.449	566	1.218	0.00264
6	3	6.488	530	0.300	0.00065
6	4	6.516	713	0.318	0.00068
10	1	6.062	937	0.716	0.00165
10	2	6.156	849	0.267	0.00061
10	3	6.193	611	0.574	0.00130
10	4	6.192	793	0.282	0.00064

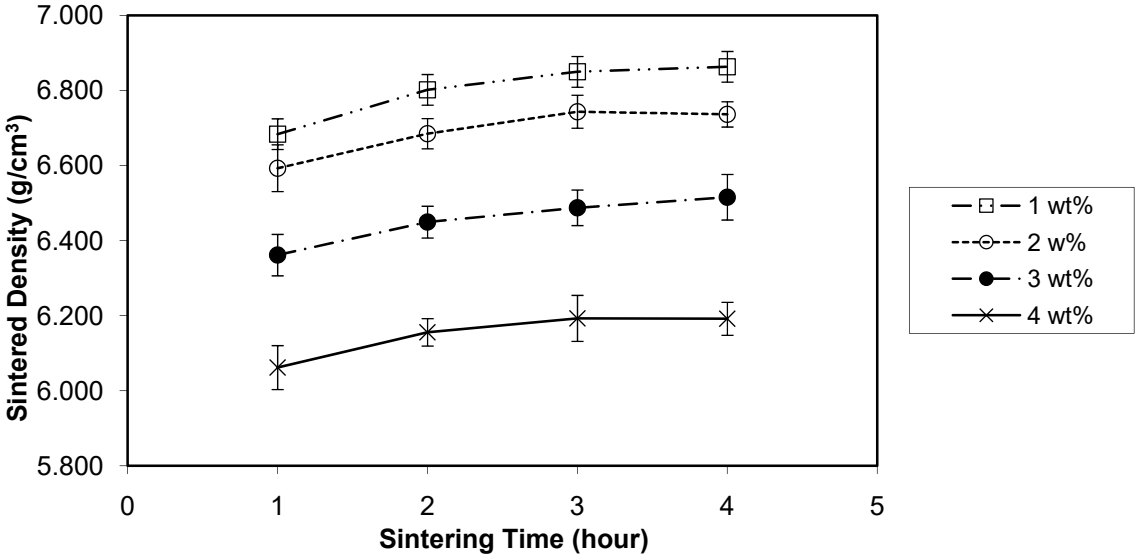

Figure 4. Sintered density of copper alumina against sintering time for the four percentages of alumina.

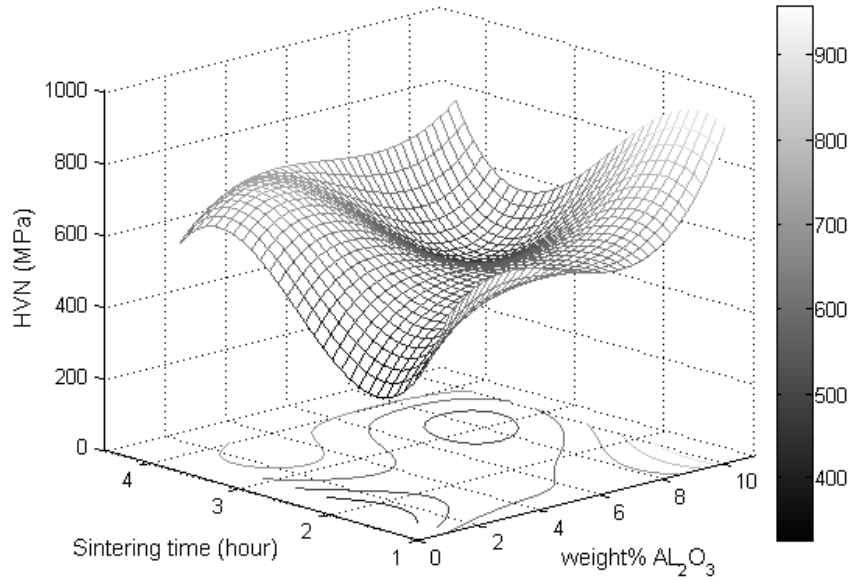

Figure 5. Vickers hardness of copper alumina against weight percentage of alumina and sintering time.

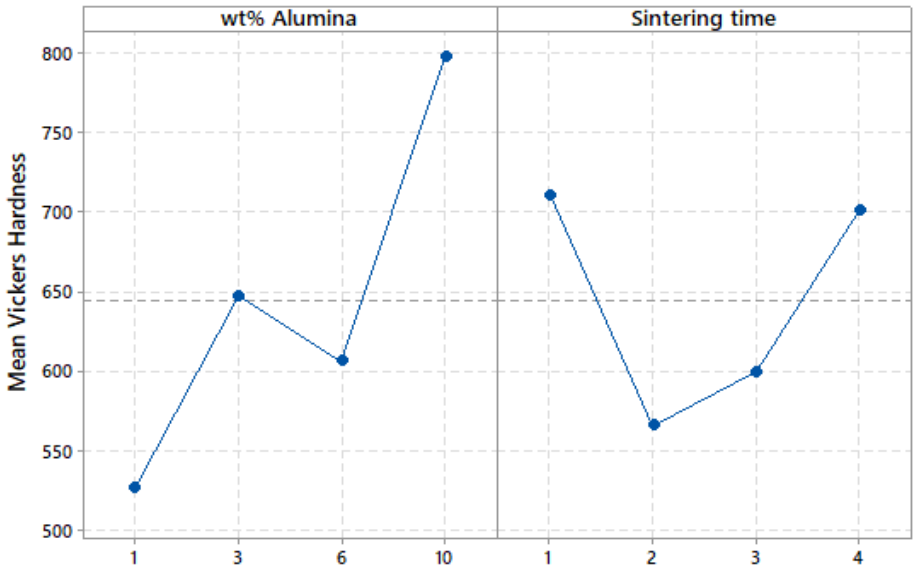

Figure 6. Main effect plot for Vickers hardness.

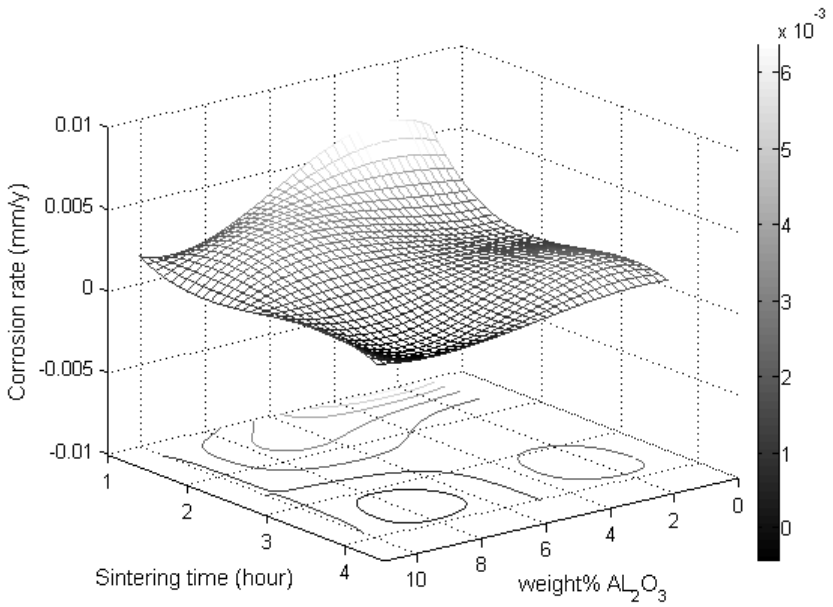

Figure 7. Corrosion rate of copper alumina against weight percentage of alumina and sintering time.

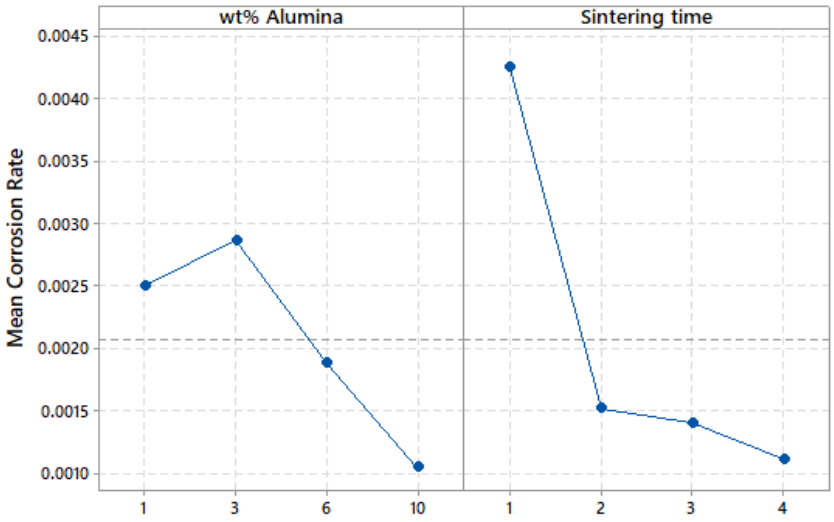

Figure 8. Main effect plot for corrosion rate.

3.1. Analysis of variance

The results presented in Figures 5–8 are based on the data mean values, but do not include confidence levels. This requires statistical analysis of the variability that exists in the data based on the ANOVA approach. This also requires a statistical model to be developed that relates the hardness and corrosion rate to the studied factors, i.e. alumina weight percentage and sintering time. Thus, the commonly used "general full factorial" linear statistical model was deployed according to Eq 4 as:

$$y_{ijk} = \mu + \tau_i + \beta_j + \in_{ijk}, \begin{cases} i = 1,2,3,4 \\ j = 1,2,3,4 \\ k = 1,2,3 \end{cases} \tag{4}$$

Where:

y_{ijk} is the response variable denoting the ijk^{th} observation of either the Vickers hardness or corrosion rate

μ is the overall mean for y_{ijk}

τ_i is the effect of the i^{th} level of alumina weight percentage on the response variable

β_j is the effect of the j^{th} level of sintering time on the response variable

$\in_{ijk}$ is the ijk^{th} error term, which is assumed as normally and independently distributed

The estimated values of the response variable (denoted $\hat{y}_{ijk}$) can be obtained using the Least Squares Method (LSM) ([26]) from Eq 5 as:

$$\hat{y}_{ijk} = \frac{1}{12}\sum_{j=1}^{4}\sum_{k=1}^{3} y_{ijk} + \frac{1}{12}\sum_{i=1}^{4}\sum_{k=1}^{3} y_{ijk} - \frac{1}{48}\sum_{i=1}^{4}\sum_{j=1}^{4}\sum_{k=1}^{3} y_{ijk} \tag{5}$$

In light of the model described by Eq 4, ANOVA can be applied by partitioning the total variability in the data into the core sources of variability: i.e. effect of the alumina concentration,

effect of the sintering time, and the error. The governing equations related to ANOVA are implemented in most commercial statistical software packages, such as Minitab®, which is used in this study. The ANOVA also employs hypothesis testing techniques to help assess which of the factorial effects are significant. The results of ANOVA after being implemented in Minitab® are shown in Figure 9. This figure shows ANOVA results for both the corrosion rate (*CR*) and Vickers hardness (*HV*). The most important statistic in these results is the p-value (reads in the output as P), which corresponds to a factorial effect that is significant if it is very small (i.e., if p-value < α, where 100(1–α)% represents the significance level) [27]. Assuming a significance level of 95% (α = 0.05), this indicates that alumina concentration has a significant effect on hardness (p-value = 0.022), but little effect on corrosion rate (p-value = 0.135). On the other hand, sintering time evidently has a significant effect on corrosion rate (p-value = 0.006), but not on hardness (p-value = 0.160). Another important statistic in the ANOVA results is the coefficient of determination or R^2 (reads as R-sq). This statistic reflects the amount of variability in the data explained by the linear statistical model [28]. Given that R^2 in the case of hardness is 71.53% and in the case of corrosion rate is 77.77%, these relatively high values suggest that the linear statistical model adequately describes the relationship between hardness and corrosion rate on one side, and alumina weight percentage and sintering time on the other side, and thus justified.

ANOVA: CR, HV versus wt% Alumina, Sintering time

Factor Information

Factor	Type	Levels	Values
wt% Alumina	Fixed	4	1, 3, 6, 10
Sintering time	Fixed	4	1, 2, 3, 4

Analysis of Variance for CR

Source	DF	SS	MS	F	P
wt% Alumina	3	0.000008	0.000003	2.40	0.135
Sintering time	3	0.000026	0.000009	8.10	0.006
Error	9	0.000010	0.000001		
Total	15	0.000043			

Model Summary

S	R-sq	R-sq(adj)
0.0010283	77.77%	62.94%

Analysis of Variance for HV

Source	DF	SS	MS	F	P
wt% Alumina	3	155450	51817	5.36	0.022
Sintering time	3	63141	21047	2.18	0.160
Error	9	86982	9665		
Total	15	305573			

Model Summary

S	R-sq	R-sq(adj)
98.3091	71.53%	52.56%

Figure 9. Minitab® output for implementing ANOVA to the Vickers hardness and corrosion rate data.

3.2. Response optimization

Equation 2 combined with the data in Table 2 can be used to predict Vickers hardness or corrosion rate at any two values of alumina weight percentage and sintering time, as long as the values are within range, i.e between 1% and 10% for the alumina weight percentage and between 1 and 4 h for the sintering time. This enables to optimize the values of alumina weight percentage and sintering time at which the hardness is maximized and/or the corrosion rate is minimized. The computations were done using Minitab®, which additionally calculates confidence intervals about the estimated values of hardness and corrosion rate, as shown in Figure 10. The results in this figure are based on equal importance (importance equals 1) for the two objective functions of hardness and corrosion rate. The weight value refers to the relative importance of the target and the bounds [29]. Thus, when the weight is increased beyond a value of 1, this requires the response to move closer to the target to achieve a specific desirability. A weight value of 1 implies that the target and the bounds are equally important. Accordingly, the optimal values for Vickers hardness and corrosion rate are obtained as 854.188 and 0.0000919, respectively. These values can be achieved when the alumina weight percentage is set at 10% and sintering time is set at 4 h.

Response Optimization: CR, HV

Parameters

Response	Goal	Lower	Target	Upper	Weight	Importance
CR	Minimum		0.001	0.00631	1	1
HV	Maximum	332	937.000		1	1

Solution

Solution	wt% Alumina	Sintering time	CR Fit	HV Fit	Composite Desirability
1	10	4	0.0000919	854.188	0.929042

Multiple Response Prediction

Variable	Setting
wt% Alumina	10
Sintering time	4

Response	Fit	SE Fit	95% CI	95% PI
CR	0.000092	0.000680	(-0.001447, 0.001630)	(-0.002697, 0.002881)
HV	854.2	65.0	(707.1, 1001.3)	(587.6, 1120.8)

Figure 10. Minitab® output for implementing the response optimization to the Vickers hardness and corrosion rate data.

Since the optimal values are only point estimates of the response variables, it is advantageous to calculate the confidence intervals for them as well. As it can be seen from Figure 10, the 95% confidence interval limits about the mean Vickers hardness are given by (707.1, 1001.3), and the 95% confidence interval limits about the mean corrosion rate are given by (0, 0.00163). A zero value is used instead of the negative one (−0.001447) obtained by Minitab® since the corrosion rate cannot be less than zero, although it is not unusual to obtain a negative value from statistical estimation techniques.

Although studies related to the preparation of copper alumina composites using powder blending and sintering differ in certain aspects, the results in this work can be compared to some of these studies. For example, Korać et al. [21] prepared copper alumina composites with 1, 1.5 and 2 wt% Al_2O_3 using mechanical alloying and sintering. Their results showed that hardness decreased overall with the increase in alumina concentration, except when alumina concentration was below 1 wt%. This is in conflict with those studies that have used much higher levels of alumina content, e.g. 20 wt% [20]. In this study it was shown that hardness increases with the increase in alumina concentration. The optimal value of hardness was found at 10 wt% alumina.

3.3. Microscopic analysis

Microscopic examination was conducted for the specimens at each combination of alumina concentration and sintering time. Micrographs for four selected specimens are shown in Figures 11–14. Figures 11–13 are for specimens having 3% alumina and subjected to one, three and four hours of sintering, respectively, while Figure 14 is for a specimen having 10% alumina and subjected to four hours of sintering. The copper particles can be distinguished in these micrographs from the alumina ones based on size and color. Copper particles are generally bigger in size (due to the size difference in the raw powders) and on a gray scale are whiter in color. Figure 11 reveal that the effect of sintering on the diffusion at one-hour duration is negligible as copper particles are mostly disconnected from each other while the alumina particles are distributed in homogenously. But as sintering time increases (as the case in Figure 12), copper diffusion becomes more significant and fewer singular copper particles remain. This continues until it reaches a point where a continuous skeleton structure of copper develops, as the one in Figure 13.

Figure 13 also shows that as the copper skeleton forms, the alumina particles become uniformly distributed within the copper matrix. This is evident as some of the large copper particles break and diffuse between the alumina particles. This causes the alumina particles to partially disperse within the copper lattice, thus potentially hindering the movement of dislocations, which leads to a dispersion strengthening of the composite. This can explain the increase in hardness as sintering time increases past the two-hour duration, while below this time sintering is not effective.

The diffusion effect of copper particles is also responsible for the increase in the composite density. The sintered density was greater on average by about 3% than the green density of the specimens. This accompanies a decrease in the effective external surface area of the composite, which in turn decreases the attack rate by the hydrochloric acid in the corrosion tests. Besides, as alumina particles tend to be enveloped by copper due to diffusion, the access to alumina by HCl is reduced. Knowing that alumina acts as cathode in corrosion due its higher electrode potential compared to copper, its presence is needed for corrosion to occur. Since sintering causes alumina to be less of reach by HCl as its time increases, therefore corrosion rate tends to decrease as sintering time increases.

As for the effect of alumina concentration, results showed that the higher the alumina content is the better the hardness and corrosion resistance will be. The increase in hardness can be explained by the dispersion strengthening effect mentioned above. Referring to Figure 14, one notes that alumina agglomerates at 10% alumina in larger quantities than that at 3% alumina (see Figure 13). Comparing between Figures 13 and 14, it can also be noted that diffusion is much more significant in Figure 13 than in Figure 14, although the sintering time is similar in both cases (three hours). It can

be inferred from this that the increase in alumina concentration tends to restrain copper diffusion, partially due to the agglomeration of alumina. Besides, regions of alumina agglomerates are richer in porosity and voids due to the lack of diffusion among these hard particles. This may contribute to increasing the composite porosity as alumina concentration increases [30]. The increase in corrosion resistance with higher alumina concentration may be attributed to the increase in the overall electrical resistivity (ρ) of the composite, where the electrical resistivity for alumina ($\rho = 1 \times 10^{12}$ Ω·m) is much higher than that for copper ($\rho = 1.68 \times 10^{-8}$ Ω·m) [31]. As the electrons need to flow along the many cathodic and anodic sites for the electrochemical corrosion to occur, the flow rate of electrons will then be slowed by the more resistive alumina.

The micrographs of Figures 11–14 reveal no sign of a third phase resulting from a chemical reaction between copper and alumina. This agrees with [32], which showed that no reaction may take place between copper and alumina during the sintering stage when the temperature is set at or below 900 °C. According to [33], copper can react with α-alumina at temperatures above 950 °C. Nevertheless, copper and alumina strongly bond together without a chemical reaction between them; likely due to van der Waals interaction [32]. The presence of oxygen at high concentration may form oxides that adversely affect the bonding between copper and alumina. However, small concentrations of oxygen happened to promote this type of bonding. Since sintering was carried out in a furnace with normal air, it is expected that oxygen was widely accessible in the composite, which causes cuprous oxides to form. Higher alumina presence may thus decrease the amount of cuprous oxides that may form. Both porosity and cuprous oxides have a negative impact on the composite strength/hardness since they reduce the total area of contact between the copper and alumina particles.

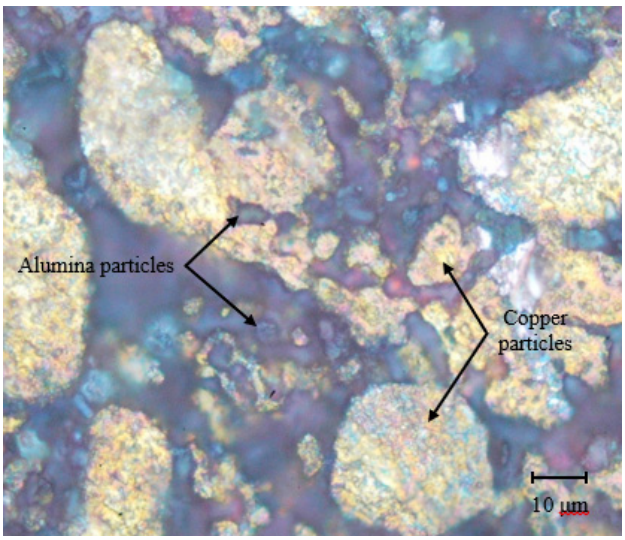

Figure 11. Optical image of a copper alumina specimen containing 3% Al_2O_3 and sintered for one hour.

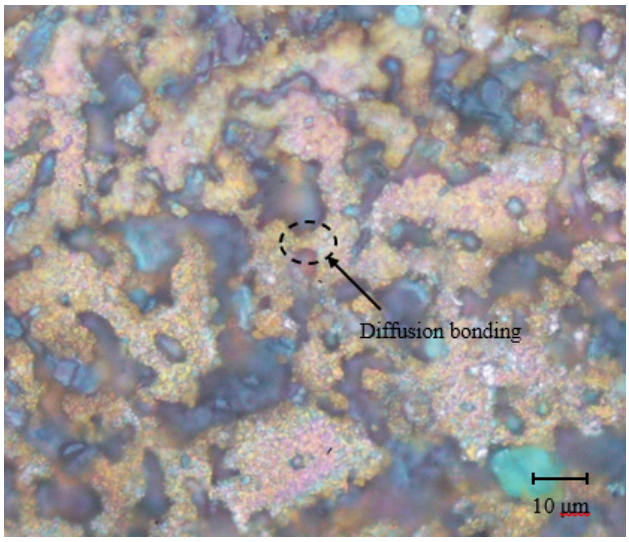

Figure 12. Optical image of a copper alumina specimen containing 3% Al_2O_3 and sintered for three hours.

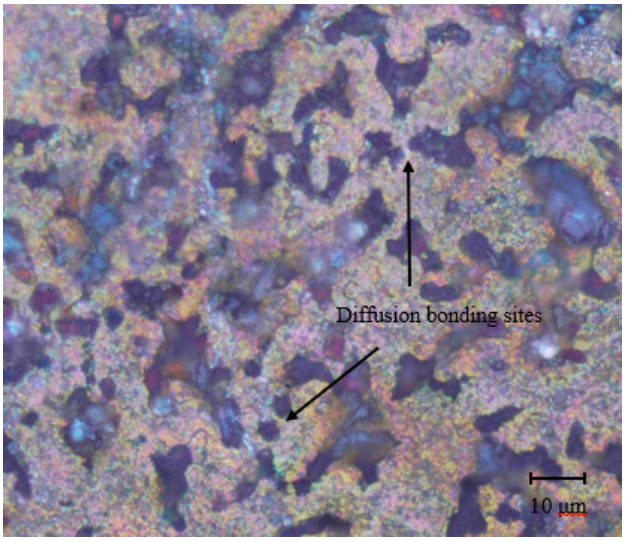

Figure 13. Optical image of a copper alumina specimen containing 3% Al_2O_3 and sintered for four hours.

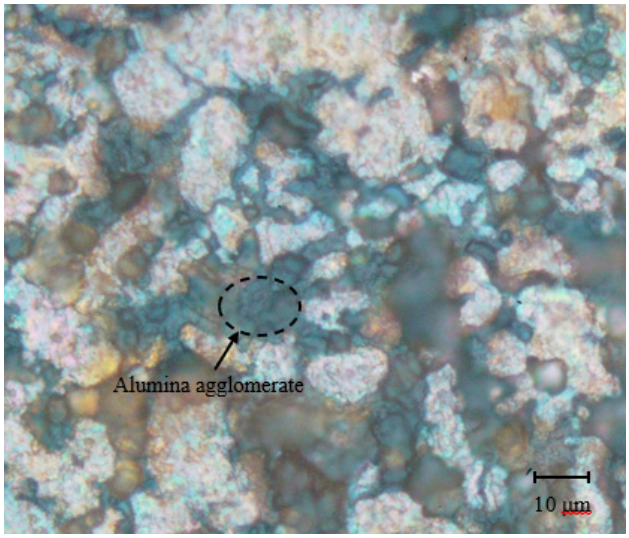

Figure 14. Optical image of a copper alumina specimen containing 10% Al_2O_3 and sintered for three hours.

4. Conclusions

In light of the results presented in this study, it can be inferred that the corrosion rate in copper alumina is reduced as either the sintering time or alumina concentration increases. Alumina concentration has a significant effect on hardness as Vickers hardness increased with alumina concentration by about 50%. However, hardness increases with sintering time only after two hours. Optimizing Vickers hardness and corrosion rate according to the statistical model developed in this study with the aid of Minitab®, it was found that the optimal values of Vickers hardness and corrosion rate can be reached when the alumina concentration and sintering time are set at 10 wt% and 4 h. The corresponding values for Vickers hardness and corrosion rate were obtained as 854.188 MPa and 0.0000919 mm/y, respectively.

The microscopic examination revealed that the addition of alumina to the copper matrix had a dispersion strengthening effect on the microstructure, which was further enhanced with sintering. The dispersion strengthening was responsible for the increase in hardness of the composite as alumina concentration increased. In addition, sintering led to the formation of a continuous skeleton structure of copper in which the alumina particles were dispersed. Corrosion rate was consequently decreased due to the decrease in the total effective surface area that can be attacked by the hydrochloric acid in the corrosion tests.

Conflict of interest

The authors declare no conflict of interest.

References

1. Alem SAA, Latifi R, Angizi S, et al. (2020) Microwave sintering of ceramic reinforced metal matrix composites and their properties: a review. *Mater Manuf Process* 35: 303–327.
2. Sankar S, Naik AA, Anilkumar T, et al. (2020) Characterization, conductivity studies, dielectric properties, and gas sensing performance of in situ polymerized polyindole/copper alumina nanocomposites. *J Appl Polym Sci* 137: 49145.
3. Singh G, Singh S, Singh J, et al. (2020) Parameters effect on electrical conductivity of copper fabricated by rapid manufacturing. *Mater Manuf Process* 1–12.
4. Asano K (2015) Preparation of alumina fiber-reinforced aluminum by squeeze casting and their machinability. *Mater Manuf Process* 30: 1312–1316.
5. Strojny-Nędza A, Pietrzak K, Gili F, et al. (2020) FGM based on copper–alumina composites for brake disc applications. *Arch Civ Mech Eng* 20: 83.
6. Mohamad SNS, Mahmed N, Halin DSC, et al. (2019) Synthesis of alumina nanoparticles by sol-gel method and their applications in the removal of copper ions (Cu^{2+}) from the solution. *IOP Conf Ser: Mater Sci Eng* 701: 12034.
7. Tang Y, Qiu S, Li M, et al. (2017) Fabrication of alumina/copper heat dissipation substrates by freeze tape casting and melt infiltration for high-power LED. *J Alloy Compd* 690: 469–477.
8. Duan L, Jiang H, Zhang X, et al. (2020) Experimental investigations of electromagnetic punching process in CFRP laminate. *Mater Manuf Process* 1–12.
9. Sang K, Weng Y, Huang Z, et al. (2016) Preparation of interpenetrating alumina–copper composites. *Ceram Int* 42: 6129–6135.
10. Winzer J, Weiler L, Pouquet J, et al. (2011) Wear behaviour of interpenetrating alumina–copper composites. *Wear* 271: 2845–2851.
11. Rakoczy J, Nizioł J, Wieczorek-Ciurowa K, et al. (2013) Catalytic characteristics of a copper–alumina nanocomposite formed by the mechanochemical route. *React Kinet Mech Cat* 108: 81–89.
12. Rajesh kumar L, Amirthagadeswaran KS (2019) Corrosion and wear behaviour of nano Al_2O_3 reinforced copper metal matrix composites synthesized by high energy ball milling. Particulate Science and Technology 1–8.
13. Eddine WZ, Matteazzi P, Celis JP (2013) Mechanical and tribological behavior of nanostructured copper-alumina cermets obtained by pulsed electric current sintering. *Wear* 297: 762–773.
14. Mohammadi E, Nasiri H, Khaki JV, et al. (2018) Copper-alumina nanocomposite coating on copper substrate through solution combustion. *Ceram Int* 44: 3226–3230.
15. Wang X, Ma J, Maximenko A, et al. (2005) Sequential deposition of copper/alumina composites. *J Mater Sci* 40: 3293–3295.
16. Lim JD, Susan YSY, Daniel RM, et al. (2013) Surface roughness effect on copper–alumina adhesion. *Microelectron Reliab* 53: 1548–1552.
17. Qiao Y, Cai X, Zhou L, et al. (2018) Microstructure and mechanical properties of copper matrix composites synergistically reinforced by Al_2O_3 and CNTs. *Integr Ferroelectr* 191: 133–144.
18. Sadoun A, Ibrahim A, Abdallah AW (2020) Fabrication and evaluation of tribological properties of Al_2O_3 coated Ag reinforced copper matrix nanocomposite by mechanical alloying. *J Asian Ceram Soc* 8: 1228–1238.

19. Rajkovic V, Bozic D, Stasic J, et al. (2014) Processing, characterization and properties of copper-based composites strengthened by low amount of alumina particles. *Powder Technol* 268: 392–400.
20. Yousif AA, Moustafa SF, El-Zeky MA, et al. (2003) Alumina particulate/Cu matrix composites prepared by powder metallurgy. *Powder Metall* 46: 307–311.
21. Korać M, Kamberović Ž, Anđić Z, et al. (2010) Sintered materials based on copper and alumina powders synthesized by a novel method. *Sci Sinter* 42: 81–90.
22. Zheng Z, Li XJ, Gang T (2009) Manufacturing nano-alumina particle-reinforced copper alloy by explosive compaction. *J Alloy Compd* 478: 237–239.
23. Yousefieh M, Shamanian M, Arghavan AR (2012) Analysis of design of experiments methodology for optimization of pulsed current GTAW process parameters for ultimate tensile strength of UNS S32760 welds. *Metallogr Microstr Anal* 1: 85–91.
24. Bataineh O, Al-shoubaki A, Barqawi O (2012) Optimising process conditions in MIG welding of aluminum alloys through factorial design experiments. *Latest Trends in Environmental and Manufacturing Engineering Optimising* 21–26.
25. Thiraviam R, Sornakumar T, Senthil Kumar A (2008) Development of copper: alumina metal matrix composite by powder metallurgy method. *Int J Mater Prod Tec* 31: 305–313.
26. Montgomery DC (2017) *Design and Analysis of Experiments*, 9 Eds., Hoboken: John Wiley & Sons.
27. Bataineh O (2019) Effect of roller burnishing on the surface roughness and hardness of 6061-T6 aluminum alloy using ANOVA. *IJMERR* 8: 565–569.
28. Bataineh O, Dalalah D (2010) Strategy for optimising cutting parameters in the dry turning of 6061-T6 aluminium alloy based on design of experiments and the generalised pattern search algorithm. *IJMMM* 7: 39–57.
29. Equbal MI, Equbal A, Mukerjee D (2018) A full factorial design-based desirability function approach for optimization of hot forged vanadium micro-alloyed steel. *Metallogr Microsta Anal* 7: 504–523.
30. Almomani MA, Tyfour WR, Nemrat MH (2016) Effect of silicon carbide addition on the corrosion behavior of powder metallurgy Cu–30Zn brass in a 3.5 wt% NaCl solution. *J Alloy Compd* 679: 104–114.
31. Michálek M, Sedláček J, Parchoviansky M, et al. (2014) Mechanical properties and electrical conductivity of alumina/MWCNT and alumina/zirconia/MWCNT composites. *Ceram Int* 40: 1289–1295.
32. Yoshino Y (1989) Role of oxygen in bonding copper to alumina. *J Am Ceram Soc* 27: 1322–1327.
33. Hu W, Donat F, Scott SA, et al. (2016) The interaction between CuO and Al_2O_3 and the reactivity of copper aluminates below 1000 °C and their implication on the use of the Cu–Al–O system for oxygen storage and production. *RSC Adv* 6: 113016–113024.